FEBS Letters 455 (1999) 332–338 FEBS 22340

Molecular dynamics simulation of a synthetic four-α-helix bundle that binds the anesthetic halothane

Lowri A. Davies[a], Michael L. Klein[a,*], Daphna Scharf[b]

[a] *Center for Molecular Modeling, Department of Chemistry, University of Pennsylvania, Philadelphia, PA 19104-6323, USA*
[b] *Department of Anesthesia, University of Pennsylvania Medical Center, Philadelphia, PA 19104-4283, USA*

Received 30 April 1999; received in revised form 17 June 1999

Abstract The structural features of binding sites for volatile anesthetics are examined by performing a molecular dynamics simulation study of the synthetic four-α-helix bundles $(A\alpha_2)_2$, which are formed by association of two 62-residue di-α-helical peptides. The peptide bundle $(A\alpha_2)_2$ was designed by Johansson et al. [Biochemistry 37 (1998) 1421–1429] and was shown experimentally to have a high affinity for the binding of the anesthetic halothane ($CF_3CBrClH$) in a hydrophobic cavity. Since $(A\alpha_2)_2$ can exhibit either the *anti* or *syn* topologies, the two distinct bundles are simulated both in the presence and in the absence of halothane. Nanosecond length molecular dynamics trajectories were generated for each system at room temperature ($T = 298$ K). The structural and dynamic effects of the inclusion of halothane are compared, illustrating that the structures are stable over the course of the simulation; that the $(A\alpha_2)_2$ bundles have suitable pockets that can accommodate halothane; that the halothane remains in the designed hydrophobic cavity in close proximity to the Trp residues with a preferred orientation; and that the dimensions of the peptide are perturbed by the inclusion of an anesthetic molecule.

Key words: Molecular dynamics simulation; Synthetic four-α-helix bundle; Halothane

1. Introduction

The distinct in vivo molecular targets for inhaled general anesthetic action remain unknown despite decades of research. Ambiguity persists in the relative roles of lipids and proteins in the mechanism of anesthesia, and in the existence of specific versus non-specific binding sites for inhaled anesthetics [1–3]. Quantitative considerations have tilted the focus in recent years to membrane-bound proteins, in particular to trans-membrane ion channels [4–8]. Current interest lies in the understanding of the properties and structural features of anesthetic binding sites in proteins. Numerous spectroscopic studies have illustrated that specific, discrete sites exist in both water-soluble proteins and membrane-bound proteins, where anesthetics may bind [9–17]. These sites are predominately hydrophobic in character but also have hydrophilic, polar components [18–20]. Uncertainty still exists in the exact relation between critical amino acids and the potential anesthetic binding sites [3]. In the reconstituted $GABA_A$ receptor, for example, a number of amino acids in the sequence were suggested to control the gating response observed in the presence of anesthetics [21].

The complex nature of membrane-bound proteins motivated a novel approach to study their properties by using synthetic peptides with known amino acid sequences, which are representative of the lipid-spanning domain of native structures [22,23]. Such synthetic designed peptides may exhibit specific binding for anesthetics [24,25]. More recently Johansson et al. have designed a synthetic peptide, $(A\alpha_2)$, which in dimeric form specifically binds the inhaled anesthetic halothane ($CF_3CBrClH$) with high affinity [26]. The dimer $(A\alpha_2)_2$ consists of two 62-residue segments, each containing two 27-residue α-helical stretches connected by an eight-residue Gly loop linker. The two monomers associate into a water-soluble four-α-helix bundle with a hydrophobic core containing two Trp residues. The binding of halothane to the hydrophobic interior of the $(A\alpha_2)_2$ bundle is inferred experimentally from the quenching of the Trp fluorescence spectrum. Since fluorescence quenching by heavy atoms occurs over distances of less than 3–5 Å [27,28], the halothane molecule is likely to be located in close proximity to one (or both) of the core Trp residues.

Two possible topologies exist for the dimer $(A\alpha_2)_2$, either *anti* [29,30] or *syn* [31,32]. When a spin label is attached to the Cys residues within the hydrophobic core of $(A\alpha_2)_2$, the *anti* topology is predominant ($>99\%$) in water [26]. However, since the size of the spin label is large, it remains open to question whether the *anti* topology is favored for the $(A\alpha_2)_2$ bundle without the spin label.

A description of the interactions between halothane and the four-α-helix structure, and of the relative orientation of the anesthetic molecule with respect to specific residues in the hydrophobic core cannot be obtained from experimental studies such as [26]. The favorable interactions between halothane and the interior of the $(A\alpha_2)_2$ suggest that suitable hydrophobic interior pockets for the anesthetic have been achieved by the peptide design. Molecular dynamics (MD) simulations can examine structure stability, interactions and molecular motions that occur on nanosecond time scales. The use of MD simulations to probe the structural and dynamic properties of biological molecules is well established and the results obtained can be used to complement experimental findings [33].

Our goal in this paper is to test the proposed design for $(A\alpha_2)_2$ by implementing MD simulation techniques. We

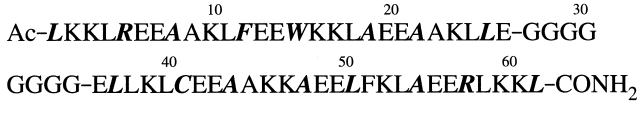

Fig. 1. Sequence of the $A\alpha_2$, the synthetic di-α-helical peptide designed to have hydrophobic residues occupying the heptad **a** and **d** positions (shown in bold italic) inside the core of the water soluble four-α-helix bundle $(A\alpha_2)_2$ [26].

*Corresponding author. Fax: (1) (215) 898 8296.
E-mail: klein@lrsm.upenn.edu

PII: S0014-5793(99)00890-X

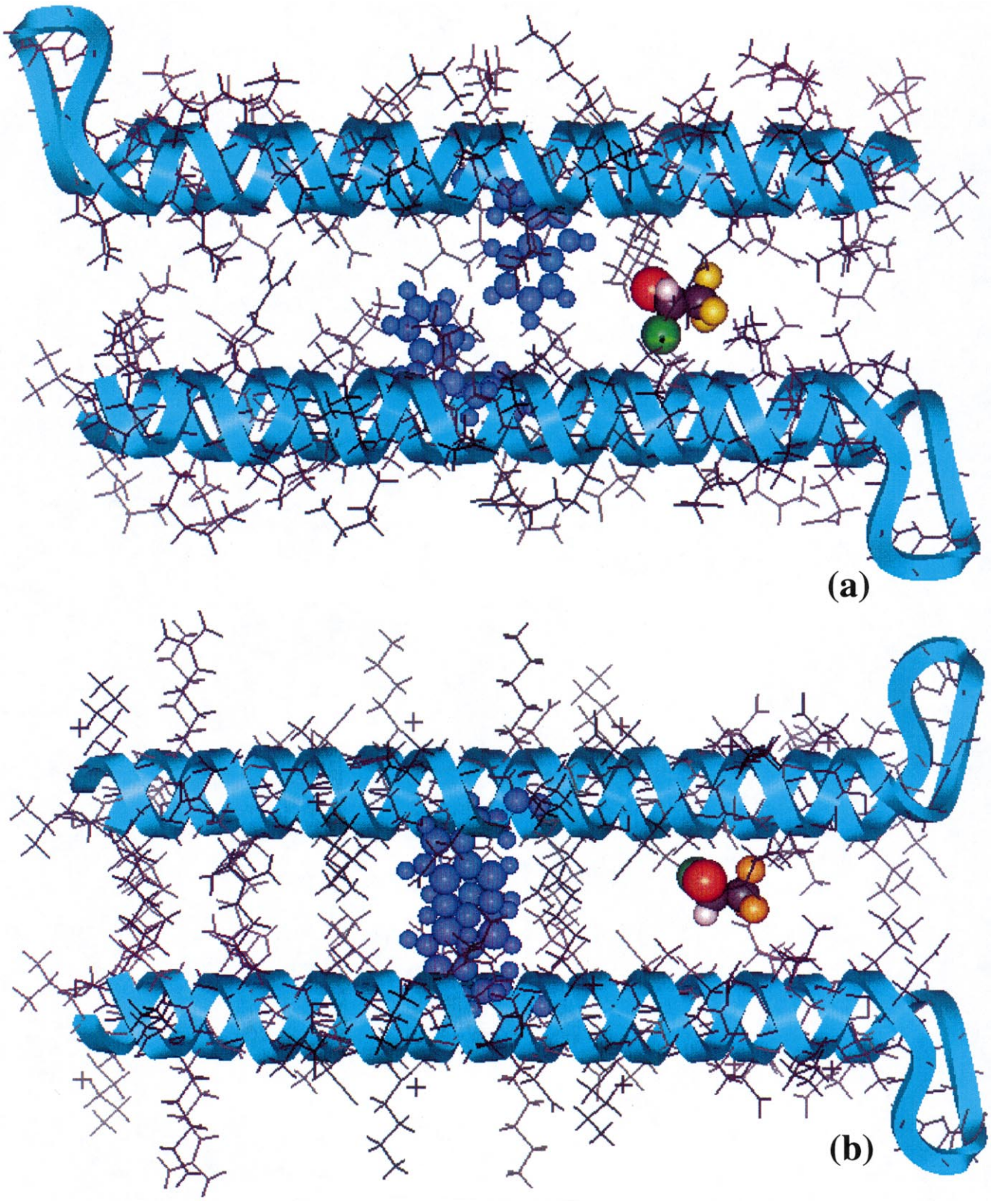

Fig. 2. Initial configurations of the $(A\alpha_2)_2$ four-α-helix bundles used in the simulations, in (a) *anti* and (b) *syn* topologies, both in the presence of halothane. The four helices are shown in light blue ribbon rendering with the amino acid side chains in sticks, the interior Trp residues shown in dark blue, the carbon atoms of the halothane molecule are in gray, its fluorine atoms in yellow, bromine atom in orange and chlorine in green.

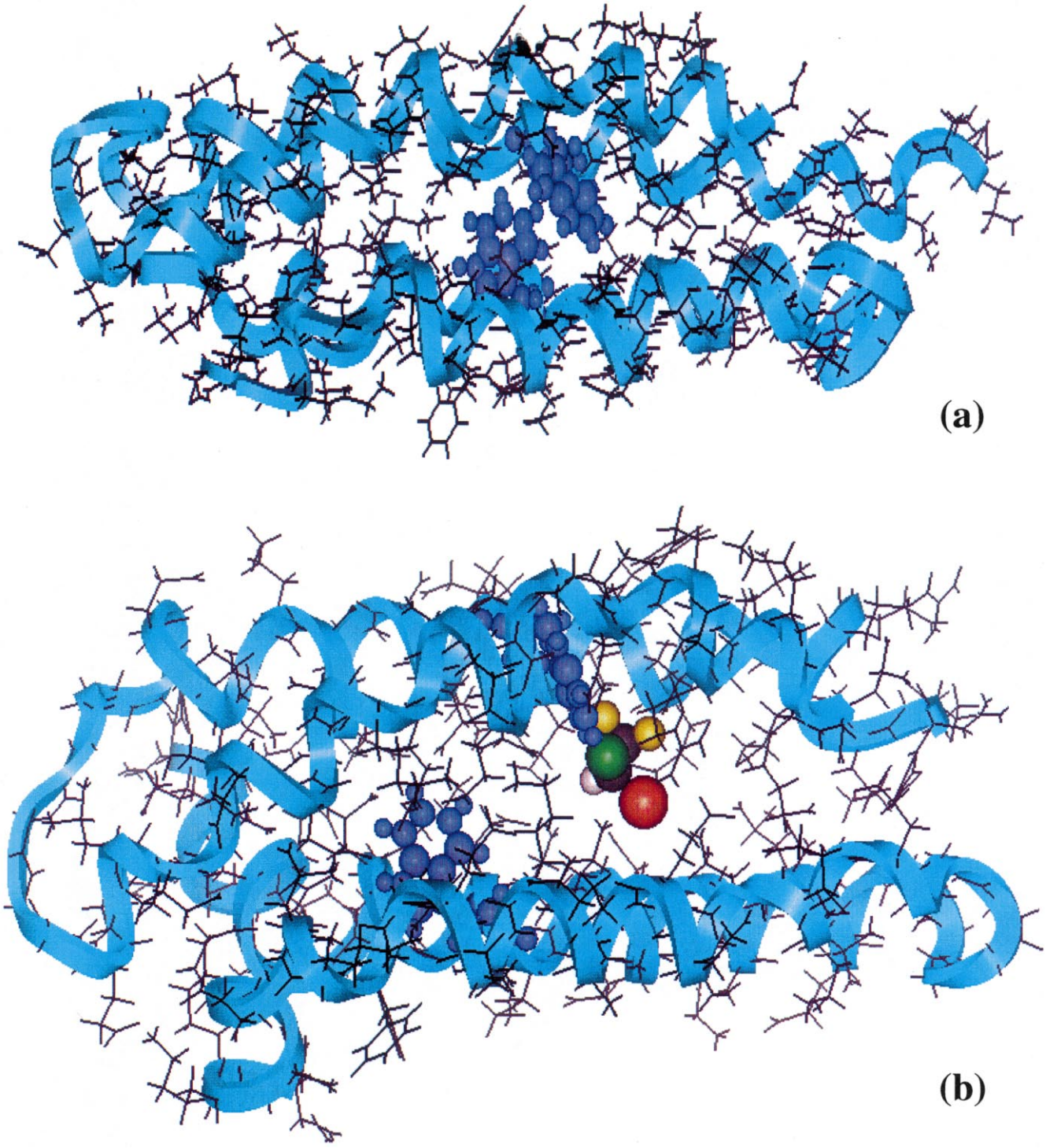

Fig. 3. Average configurations for the *anti* topology of the synthetic $(A\alpha_2)_2$ four-α-helix peptide bundle $(A\alpha_2)_2$ obtained over the last 500 ps of the simulation, in the absence (a) and in the presence (b) of halothane. See Fig. 2 for color code.

present the results of MD simulation studies of the four-α-helix bundle $(A\alpha_2)_2$ in both the *anti* and *syn* topologies, each in the presence and absence of a single halothane molecule. Specifically, we examine the stability of the designed $(A\alpha_2)_2$ structures and the ability of the associated bundles to yield suitable hydrophobic cores, which can accommodate halothane in close proximity to the Trp residues. We concentrate on structural consequences and modifications to the $(A\alpha_2)_2$ bundles upon addition of the anesthetic halothane, the dynamics and relative orientation of the halothane in the proposed cavities.

2. Simulation system and methodology

The initial coordinates for the di-α-helical monomer $A\alpha_2$ were obtained using InsightII software (Molecular Simulation

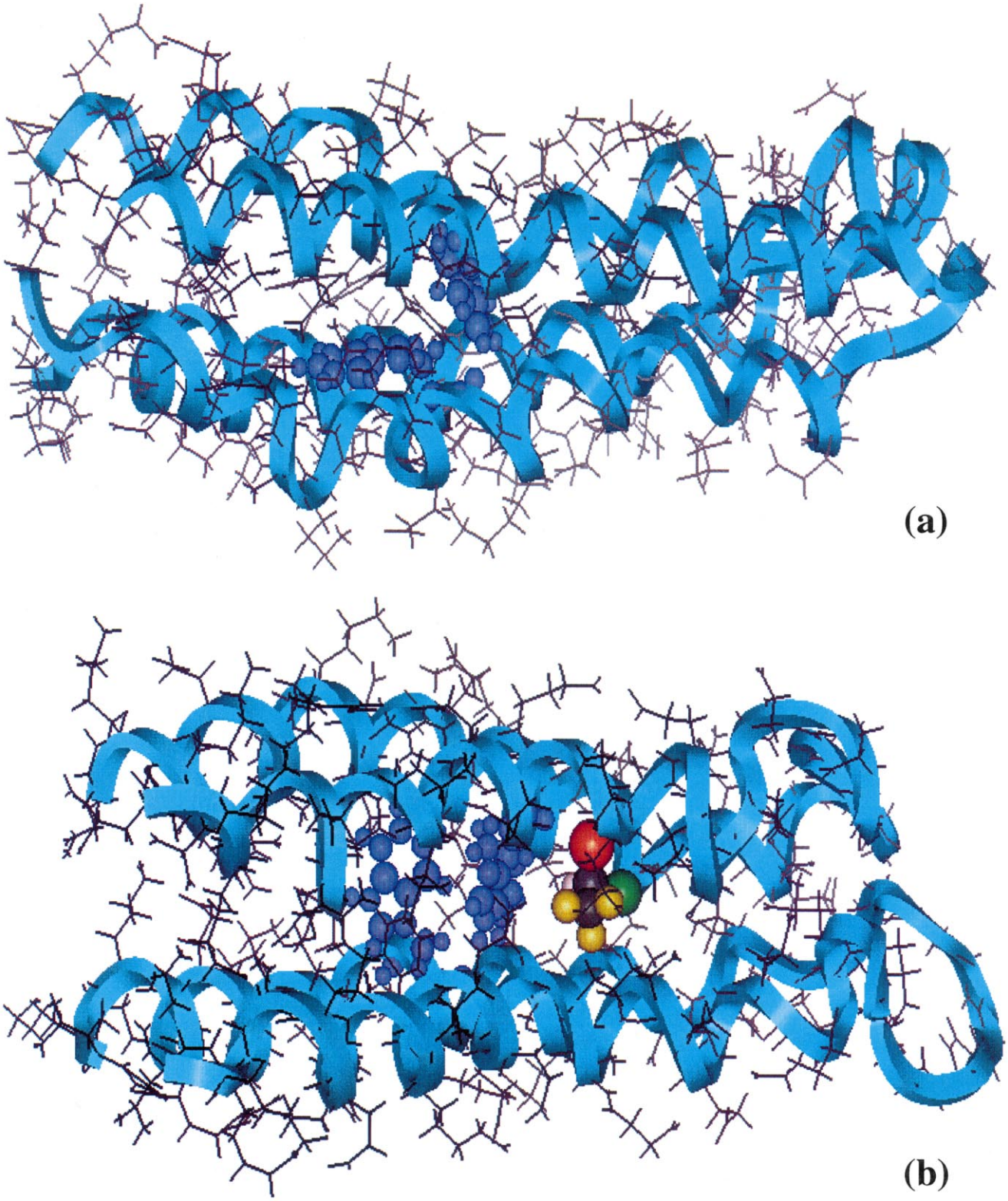

Fig. 4. Average configurations for the *syn* topology of the synthetic $(A\alpha_2)_2$ four-α-helix peptide bundle $(A\alpha_2)_2$ obtained over the last 500 ps of the simulation, in the absence (a) and in the presence (b) of halothane. See Fig. 2 for color code.

Inc., San Diego, CA, Version 97.2) by constructing ideal right-handed α-helices using the amino acid sequence given in [26], see also Fig. 1. The four-α-helix bundle was formed by placing two of these monomers together in either the *anti* or *syn* topology. Care was taken to ensure that none of the side chain atoms in the structure were overlapping, but the monomers were placed close enough so that interactions could easily occur between residues of the two monomers. The hydrophobic side chains were thus initially within the core of the four-α-helix structure. When the anesthetic was included in

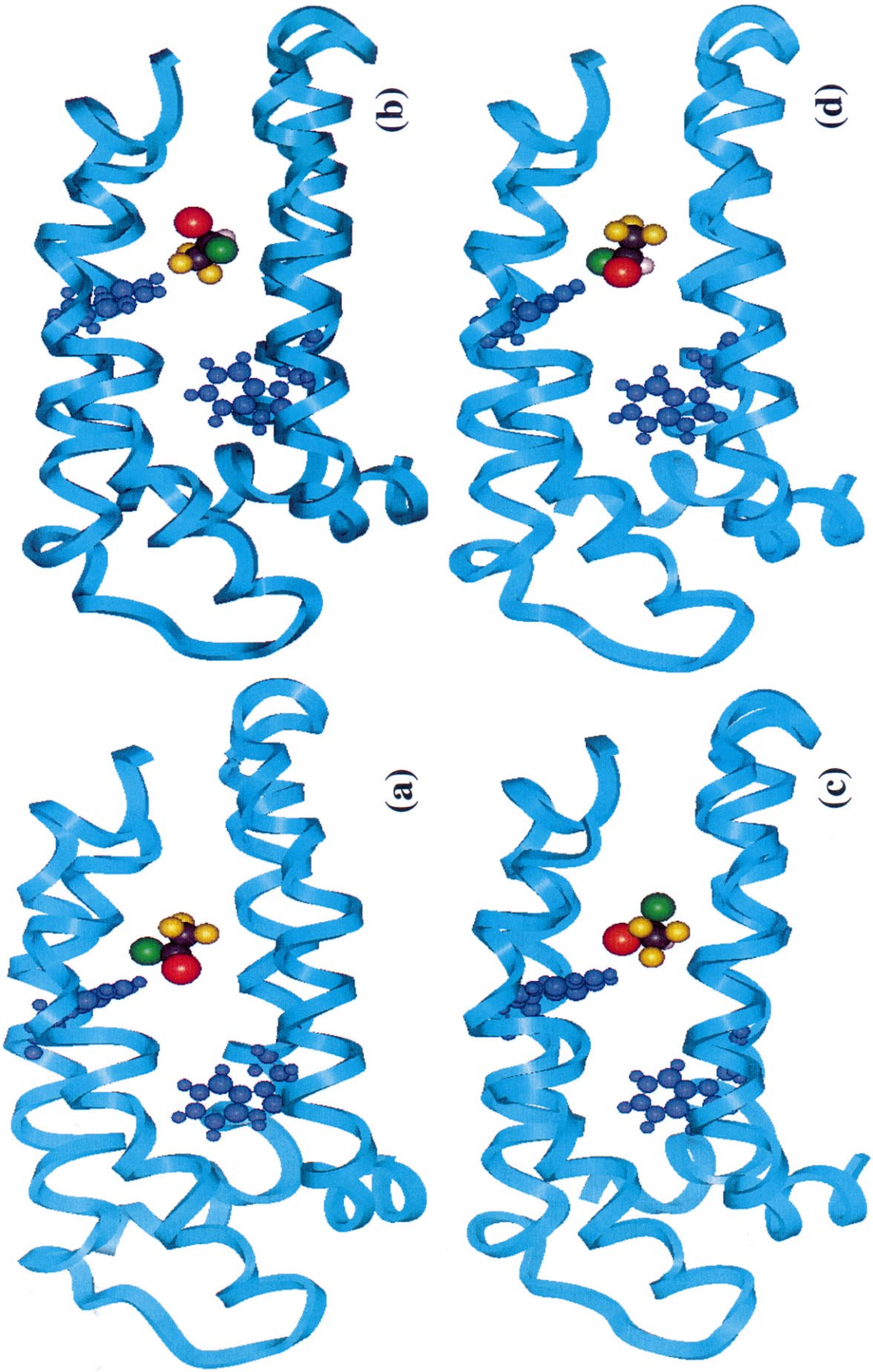

Fig. 5. Snapshots from the simulation for the *anti* topology of the $(A\alpha_2)_2$ peptide bundle with halothane, illustrating different possible orientations (a–d) of the halothane with respect to one of the Trp residues. See Fig. 2 for color code, the side chains of the peptide were eliminated for clarity.

the system, a single halothane molecule (also constructed using InsightII) was placed in a cavity within the hydrophobic core of the synthetic peptide. No anesthetic and the protein atoms were less than 1.6 Å apart, see Fig. 2. The halothane molecule was placed in an orientation such that its carbon-carbon axis was parallel to the long axis of the four helices, with the di-halogenated carbon atom closest to the Trp residues in the core. In the *anti* topology the two hydrophobic cavities above and below the Trp residues are equivalent, but in the case of the *syn* topology two distinct locations for the halothane exist; in our simulation of the *syn* topology we initially place the anesthetic molecule in the cavity between the two Trp residues and the Gly loop region.

Minimizations of each structure were performed using a steepest descent algorithm in CHARMM [34] with the helix backbone atoms initially constrained and then with all the atoms free to move. All unfavorable interactions within these initial structures were thus removed. The potential energy function for the dynamics of each of the four bundles was then constructed using the AMBER-95 parameter set [35–37], where the empirical form of the energy expression is given as a sum of inter- and intra-molecular interactions. The inter-molecular portion consists of van der Waals interactions which are repulsive at very short distances and attractive at larger separations, and an electrostatic contribution, which accounts for the interactions between charged species. The intra-molecular component contains contributions due to bond stretching, bond-angle bending and bond torsions. For halothane we use interaction parameters from [38]. The standard Lorenz-Berthelot combining rules were used to calculate the cross interactions between the peptide and halothane.

The extended system simulation method of the PINY-MD computational package [39,40] was used to obtain constant *NVT* MD trajectories for the four synthetic peptide systems. In this initial study no explicit solvent is used. The standard periodic boundary conditions and minimum image conventions are incorporated into this approach, and Nosé-Hoover thermostat chains of length $m = 2$ maintain a constant system temperature of $T = 298$ K. Electrostatic interactions are calculated using the particle-mesh Ewald technique [41]. All bonds to hydrogen atoms were constrained to their equilibrium values during the simulation using the SHAKE and RATTLE algorithms. The unit cell of the simulation consisted of a rectangular box of size 40 Å × 40 Å × 60 Å, where the long axis of the four-α-helix structure was placed parallel to the long box axis.

Four individual simulations of the synthetic four-α-helix bundles were performed; one with the $A\alpha_2$ peptide monomers in an *anti* topology; another with the monomers in a *syn* topology; and two more with the *anti* and *syn* topologies in the presence of halothane. Each system was equilibrated in three stages: 10 ps at $T = 1$ K, 40 ps at $T = 150$ K and 50 ps at $T = 298$ K. A 1 ns trajectory was then generated for each of the four structures using a time-step of 0.5 fs at $T = 298$ K.

3. Results and discussion

At the end of 1 ns of simulation each of the four systems maintain an overall four-α-helical structure with the hydrophobic side chains in the amino acid sequence contained within the core. Some unraveling of the helices at the C and N terminals, and close to the Gly loop region is observed, together with a significant amount of bending and twisting (see Figs. 3 and 4). Following an initial period of ~200 ps the inter-helical distances reach their equilibrium values around which only small fluctuations are observed. For example, in the case of the $(A\alpha_2)_2$ peptide in the *anti* topology the four inter-helical distances are 10.71 ± 0.84 Å, 10.34 ± 0.81 Å, 11.65 ± 0.92 Å and 11.05 ± 0.87 Å, respectively.

Insight into the overall structure is obtained via a calculation of the inertia tensor of the bundles. The two components of the inertia tensor in the plane perpendicular to the long axis of the helices are decreased in both the *anti* and *syn* topologies when halothane is present in the hydrophobic core, indicating that the structures are more swollen in the presence of anesthetic. Conversely, the component of the inertia tensor parallel to the long axis of the helices increases upon addition of halothane, which corresponds to a decrease in the overall length of the four-α-helices. This effect is most apparent for the *anti* topology. The deformation of the structure due to the presence of halothane is illustrated further by monitoring the average lengths of the four-α-helices during the simulation. In both the *anti* and *syn* topologies addition of halothane is found to decrease this average end-to-end helix distance, which is manifest even after the CHARMM minimization. The difference between the results obtained for the systems with and without the anesthetic is again more pronounced in the *anti* topology of the $(A\alpha_2)_2$ four-helix bundle.

In addition to the overall structural modifications to the four-α-helix bundle due to the anesthetic, other interesting effects can be observed via a more detailed study of the dynamic behavior of the halothane molecule. During the simulations, for both the *anti* and *syn* topologies, the halothane molecule is confined into the small region within the hydrophobic core of the peptide structure where it was initially placed. The absence of any large-scale migration of the anesthetic is to be expected due to the relatively short (nanosecond) time scale of the simulation. However, a significant amount of rotational and translational motion of halothane is observed inside the cavity, the net effect of which is motion towards the Trp residues. In particular, the distance between the two Trp residues within the hydrophobic core is significantly increased in the presence of halothane for the *anti* topology. The separation of these two aromatic residues is not affected by the addition of anesthetic in the *syn* topology. Halothane appears to have a favorable interaction with one Trp in the core of the *anti* topology, which draws this residue away from the vicinity of the other Trp side-chain. The lack of a similar effect in the *syn* topology could be a result of a difference in structure of the hydrophobic core region close to the Trp residues as compared to the corresponding location in the the *anti* oriented four-α-helix bundle.

Close examination of the relative orientation of the halothane molecule during the simulations of both the *anti* and *syn* topologies show that the di-halogenated carbon atom is found closest to the Trp residues. Despite having been placed in this orientation initially, the halothane molecules do rotate completely during the simulation, so that the tri-fluorinated carbon is closest to the Trp residues, see Fig. 5. However, the halothane molecules return very rapidly to their preferred orientation. This corresponds to the experimental observations of the pronounced quenching of the Trp fluorescence spectrum, which requires that the halothane halogen atoms and the Trp side chains are in close proximity.

4. Conclusions

A MD simulation study has been performed at $T = 298$ K for a synthetic four-α-helix bundle $(A\alpha_2)_2$ in two different topologies, both in the presence and in the absence of the volatile anesthetic halothane. Overall, the helical character and the position of the hydrophobic residues within the cavity of peptide bundle are all maintained on a nanosecond time scale. Occupation of the hydrophobic cavity by halothane leads to structural changes in the four-α-helix bundles, most significantly in the *anti* topology. Analysis of the motion of the halothane molecule within the cavity in the protein scaffold illustrates that the halothane exhibits a preferred orientation with respect to the Trp residues in the core, with the dihalogenated carbon closer to the core Trp residues than the tri-fluorinated carbon. This is consistent with the fluorescence quenching observed in [26]. The ability of this gas-phase simulation study, for the same peptide system, to give results which are in line with experimental findings is most gratifying. More extensive simulations, where the four-α-helix bundle is in aqueous solution are currently being performed, and preliminary results indicate that water molecules are completely excluded from the hydrophobic core of the peptide scaffold (both in the presence and absence of halothane). Thus, the absence of explicit solvent in the present work does not affect the dynamic features of the anesthetic molecule.

The use of a designed synthetic peptide to study the nature of protein-anesthetic interactions is a novel approach where experimental and simulation methods can be used in parallel to obtain a systematic analysis of the governing factors. Such studies are only able to provide insight into the structural features of the binding of halothane to the hydrophobic interior of this specific model. However, the interactions of anesthetics with hydrophobic pockets is likely to be only one of the many possible ways in which protein structure is modified in vivo.

Acknowledgements: Q.-F. Zhong, J.S. Johansson, R.G. Eckenhoff and P.L. Dutton are thanked for useful discussions. This research was supported by NIH Grant P01 GM 55876. Computer resources were provided by NPACI San Diego, CA under the auspices of MCA 93S020 and PSC Pittsburgh, PA under CHE 980006P.

References

[1] Cantor, R.S. (1999) Biophys. J. 76, May issue.
[2] Cantor, R.S. (1997) Biochemistry 36, 2339–2344.
[3] Miller, K.W. (1985) Int. Rev. Neurobiol. 27, 1–61.
[4] Forman, S.A., Miller, K.W. and Yellen, G. (1995) Mol. Pharmacol. 48, 574–581.
[5] Franks, N.P. and Lieb, W.R. (1994) Nature 367, 607–614.
[6] Franks, N.P. and Lieb, W.R. (1997) Nature 389, 334–335.
[7] Harris, R.A., Mihic, S.J., Dildy-Mayfield, J.E. and Machu, T.K. (1995) FASEB J. 9, 1454–1462.
[8] Eckenhoff, R.G. and Johansson, J.S. (1997) Pharmacol. Rev. 49, 343–367.
[9] Dubois, B.W. and Evers, A.S. (1992) Biochemistry 31, 7069–7076.
[10] Dubois, B.W., Cherian, S.F. and Evers, A.S. (1993) Proc. Natl. Acad. Sci. USA 90, 6478–6482.
[11] Xu, Y., Tang, P., Firestone, L. and Zhang, T.T. (1996) Biophys. J. 70, 532–538.
[12] Eckenhoff, R.G. and Shuman, H. (1993) Anesthesiology 79, 96–106.
[13] Eckenhoff, R.G. (1996) Proc. Natl. Acad. Sci. USA 93, 2807–2810.
[14] Johansson, J.S. and Eckenhoff, R.G. (1996) Biochim. Biophys. Acta 1290, 63–68.
[15] Raines, D.E. and McClure, K.B. (1997) Anesthesiology 86, 476–486.
[16] Johansson, J.S. (1997) J. Biol. Chem. 272, 17961–17965.
[17] Kosk-Kosicka, D., Fomitcheva, I., Lopez, M.M. and Eckenhoff, R.G. (1997) FEBS Lett. 402, 189–192.
[18] Franks, N.P. and Leib, W.R. (1978) Nature 274, 339–342.
[19] Sandorfy, C. (1978) Anesthesiology 48, 357–359.
[20] Abraham, M.H., Leib, W.R. and Franks, N.P. (1991) J. Pharm. Sci. 80, 719–724.
[21] Mihic, J.C., Ye, Q., Wick, M.J., Koltchine, V.V., Krasowski, M.D., Finn, S.E., Mascia, M.P., Valenzuela, C.F., Hanson, K.K., Greenblatt, E.P., Harris, R.A. and Harrison, N.L. (1997) Nature 389, 385–389.
[22] Lear, J.D., Wasserman, Z.R. and DeGrado, W.F. (1988) Science 240, 1177–1181.
[23] Robertson, D.E., Farid, R.S., Moser, C.C., Urbauer, J.L., Mulholland, S.E., Pidikiti, R., Lear, J.D., Wand, A.J., DeGrado, W.F. and Dutton, P.L. (1994) Nature 368, 425–432.
[24] Johansson, J.S., Eckenhoff, R.G. and Dutton, P.L. (1995) Anesthesiology 83, 316–324.
[25] Johansson, J.S., Rabanal, F. and Dutton, P.L. (1996) J. Pharmacol. Exp. Ther. 279, 56–61.
[26] Johansson, J.S., Gibney, B.R., Rabanal, F., Reddy, K.S. and Dutton, P.L. (1998) Biochemistry 37, 1421–1429.
[27] Tsao, D.H.H., Casa-Finet, J.R., Maki, A.H. and Chase, J.W. (1989) Biophys. J. 55, 927–936.
[28] Basu, G., Anglos, D. and Kuki, A. (1993) Biochemistry 32, 3067–3076.
[29] Gibney, B.R., Johansson, J.S., Rabanal, F., Skalicky, J.J., Wand, A.J. and Dutton, P.L. (1997) Biochemistry 36, 2798–2806.
[30] Grosset, A.M., Rabanal, F., Farid, R.S., Robertson, D.E., Pilloud, D.L., DeGrado, W.F. and Dutton, P.L. (1996) in: Peptides: Chemistry, Structure and Biology (Kaumaya, P.T.P. and Hodges, R.S., Eds.), pp. 573–574, Mayflower Scientific Ltd., UK.
[31] Rabanal, F., DeGrado, W.F. and Dutton, P.L. (1996) J. Am. Chem. Soc. 118, 473–474.
[32] Betz, S.F., Liebmann, P.A. and DeGrado, W.F. (1997) Biochemistry 36, 2450–2458.
[33] Karplus, K. and Petsko, G.A. (1990) Nature 347, 631–639.
[34] Brooks, B.R., Bruccoleri, R.E., Olafson, B.D., States, D.J., Swaminathan, S. and Karplus, M. (1983) J. Comp. Chem. 4, 187–217.
[35] Weiner, S.J., Kollman, P.A., Case, D.A., Singh, U.C., Ghio, C., Alagona, G., Profeta Jr., S. and Weiner, P. (1984) J. Am. Chem. Soc. 106, 765–783.
[36] Weiner, S.J., Kollman, P.A., Nguyen, D.T. and Case, D.A. (1986) J. Comp. Chem. 7, 230–235.
[37] Cornell, W.D., Cieplak, P., Bayly, C.I., Gould, I.R., Merz, K.M., Ferguson, D.M., Spellmeyer, D.C., Fox, T., Caldwell, J.W. and Kollman, P.A. (1995) J. Am. Chem. Soc. 117, 5179–5197.
[38] Scharf, D. and Laasonen, K. (1996) Chem. Phys. Lett. 258, 276–282.
[39] Martyna, G.J., Tuckerman, M.E., Tobias, D.J. and Klein, M.L. (1996) Mol. Phys. 87, 1117–1157.
[40] Martyna, G.J., Samuelson, S., Hughes, A., Tobias, D.J., Yarne, D., Klein, M.L. and Tuckerman, M.E., to be published.
[41] Darden, T., York, D. and Pedersen, L. (1993) J. Chem. Phys. 98, 10089–10092.